ELSEVIER

International Journal of Mass Spectrometry 210/211 (2001) 59–69

www.elsevier.com/locate/ijms

Ionization of 2,5-dihydroxybenzoic acid (DHB) matrix-assisted laser desorption ionization experiments and theoretical study

Sophie Bourcier, Stéphane Bouchonnet, Yannik Hoppilliard

DCMR-UMR CNRS 7651, Ecole Polytechnique, 91128 Palaiseau Cedex, France

Received 24 January 2001; accepted 25 March 2001

Abstract

The 2,5-dihydroxybenzoic acid (DHB), well known as one of the most efficient matrix-assisted laser desorption ionization (MALDI) matrices, was photoionized at different irradiances of a UV laser. Molecular orbital calculations were performed with a Becke-style 3 parameter using the Lee-Yang-Parr correlation functional density approach to estimate the thermochemical properties of DHB and showed a very good agreement with available experimental data. We report a first estimation of the electron affinity of DHB (54 kJ/mol). In a second step, the calculation method was used to evaluate the thermochemical reliability of several ionization models postulated from MALDI experiments. Among those proposed, we report the reactions, which are thermodynamically the most probable in the solid state and in the gas phase. We evaluated the energy involved in the formation of $DHB^{\cdot +}$ and $DHB^{\cdot -}$ molecular ions, $DHBH^+$ and $[DHB-H]^-$ pseudomolecular ions. The phenomenon of reduction of molecular ions was also theoretically studied as well as the role of the $DHBH^{\cdot}$ radical species. Our results on the reactivity of $DHBH^{\cdot}$ radical species show evidence of their very probable implication in molecular ion formation and of the great role played by the hydroxyl substituants in the particular efficiency of DHB as a MALDI matrix. We propose a simple thermochemical diagram showing evidence that MALDI is a very energy demanding process and that differences in efficiency between matrices should be related to their chemical structures rather than to their physical properties. (Int J Mass Spectrom 210/211 (2001) 59–69) © 2001 Elsevier Science B.V.

Keywords: Laser desorption; Ionization mechanisms; Unimolecular decompositions; 2,5-Dihydroxybenzoic acid; DFT molecular orbital calculations; Mass spectrometry

1. Introduction

Although desorption-ionization techniques are successfully applied to the analysis of biological, biochemical and industrial samples, the ionization mechanism of analytes remains not fully understood. Numerous ionization models were proposed to explain the formation or/and the transfer of ions from the condensed state to the gas phase. Models for ion formation in matrix-assisted laser desorption ionization (MALDI) mass spectrometry are summarized in a recent and excellent review by Zenobi and Knochenmuss [1]. These models (vide infra) often involve thermochemical data, which remain unavailable for most of molecules and difficult to obtain experimentally. In this work, the 2,5-dihydroxybenzoic acid (DHB), well known as one of the most efficient MALDI matrices, was photoionized at dif-

---

* Corresponding author. E-mail: yannik@dcmr.polytechnique.fr

Dedicated to Professor Nico Nibbering, one of the best mass spectrometrists in the world and certainly the most friendly.

PII S1387-3806(01)00446-8

ferent irradiances of a UV laser. We evaluated the energies required for the formation of molecular and pseudomolecular ions in function of the ionization models proposed in the literature [1]. We show that the energies required to observe such ions in the gas-phase, in both positive and negative polarities, may be evaluated with a good accuracy by means of molecular orbital calculations using the Becke-style 3 parameter using the Lee-Yang-Parr correlation functional (B3LYP) density functional approach. The thermochemical properties involved in ionization include the proton affinity of both neutral and deprotonated molecules. It is well known that (Gaussian-2) G2 and G2(MP2) (Möller Plesset 2) ab initio procedures provide excellent results for both deprotonation enthalpies and proton affinities (PA) of small molecules [2,3] and α-amino acids [4,5]. However, for molecules with several heavy atoms, these procedures require considerable computational times. That is why we tested density functional approaches, which are much less time consuming. Good results are reported for protonation and deprotonation energies, using a B3LYP density functional approach with a 6-311+G** basis set [6]. A maximum deviation of approximately 12 kJ/mol from experimental data was observed for both acidities and basicities [4,7]. In our calculations, the energies involved in the formation of molecular and pseudomolecular ions of DHB were thus computed up to the B3LYP/6-311+G(2*d*,2*p*) level. Our results allow us to estimate the energies associated with the different ionization models and to discuss their well founded on a thermochemical point of view.

2. Experimental

2.1. Materials

2,5-dihydroxybenzoic acid and isopropanol high-performance liquid chromatography grade were purchased from Sigma-Aldrich (St Quentin Fallavier, France) and used without further purification.

2.2. Laser irradiation

2.2.1. Sample preparation

2,5-dihydroxybenzoic acid was dissolved in pure isopropanol at a concentration of 10^{-2} M. 20 μL of solution were deposited onto a thin aluminized mylar foil stretched tight on a sample holder and allowed to evaporate to dryness.

2.2.2. Laser desorption mass spectra

Mass spectra were recorded on a time of flight (TOF) system constructed at the IPN (Institut de Physique Nucléaire, Orsay, France). This TOF instrument is fitted with three microchannel detectors, a photodiode, a multistop time to digital converter (CTN1S, IPN, Orsay, France) and transient recorders (Models 8828D and MM8104, Le Croy, New York, USA). This device is equipped with a nitrogen laser (model VSL-337, Laser Science Inc, Cambridge MA, USA, λ=337 nm, 3 ns/pulse). The laser energy is controlled by varying the angle of attenuation of a filter of variable opacity. The apparatus has been previously calibrated with a joulemeter so that a given angle can be related to an energy value. The maximum laser energy is 40 μJ per pulse of 3 ns, corresponding to a fluence of 1.33 10^4 W. The spectra were collected with an accelerating voltage of ±10 kV, according to the polarity of recording mode. The laser desorption (LD) spectra were acquired for a 60 s period. Time-to-mass conversion was achieved by external calibration with a CsI target: Cs_2I^+ (392.714 70 u) and Cs_3I^+ (652.524 13 u) have been taken as references.

2.3. Electron ionization mass spectra

The electron ionization (EI) spectra were recorded using a Hewlett-Packard (Les Ulis, France) HP-5972 quadrupole instrument. Two values of the ionizing electrons energy were used: 10 and 70 eV. The pressure was maintained at 10^{-5} mbar and the temperature was fixed at 80 °C.

2.4. *Ab initio calculations*

All calculations were carried out using the GAUSSIAN94 package [8]. Geometries were optimized without any symmetry constraint. Geometry optimizations and vibrational frequency calculations were carried out at the B3LYP/6-31+G** level. Final energetics of the most stable species were obtained with B3LYP/6-311+G(2*d*,2*p*) wave functions on the optimized geometries. Except otherwise stated, the relative energies mentioned in the text are those computed at the highest level of theory after correction for the thermal energies at 298 K (E_{therm}).

3. Results and discussion

Our results will be discussed by comparison with the desorption-ionization models proposed in the literature. Although it does certainly not reflect the reality, both desorption and ionization mechanisms for laser desorption-ionization (LDI) and MALDI mass spectrometry use to be considered separately, with the aim of simplifying the theoretical approach.

3.1. *Desorption models*

Several models were proposed to explain desorption under laser irradiation (for example see [9,10]. Schematically, a thermal evaporation is assumed for low laser fluences whereas higher fluences give rise to the so-called "ablation" process where a phase explosion of the overheated material occurs [11]. In MALDI experiments, the laser fluence leads to the formation and the expansion of a plume, a regime energetically between evaporation and ablation. The energy required for the desorption step is not well established but certainly depends on the sublimation energy of the solid sample and on the chemistry occurring in the condensed phase before expansion of the plume: desorption of preformed ions will clearly involve much more energy than sublimation of neutral species.

3.2. *Ionization models*

The ionization pathway remains mysterious in MALDI experiments. Although one laser pulse leads to several thousands of ions, the ions/neutrals ratio has been shown to be about 10^{-4}. In a general manner, the ions observed in the MALDI spectra of a sample M dispersed in a matrix Mat are radical ions ($M^{\cdot +}$, $M^{\cdot -}$), protonated (MH^+), and deprotonated ($[M-H]^-$) molecules, cationized molecules ($MCat^+$, Cat=Na, K,...), polymeric ions (M_nCat^+), multicharged molecules (MH_n^{n+}, $[M-nH]^{n-}$), fragment ions and matrix ions. Most of the ionization models given in the literature are presented and commented in [1]; they are summarized below. The formation of the cation radical of the matrix, by multiphoton ionization by way of

$$\mathrm{Mat} + nh\nu \rightarrow \mathrm{Mat}^{+\cdot} + e^{-} \tag{1}$$

was considered by many authors as a strong candidate for the UV-MALDI primary ionization step [12,13]. On a theoretical point of view, irradiances used in UV-MALDI or in UV-LDI are too low to allow significant absorption of more than two photons by a matrix molecule. Since the ionization energy of the commonly used matrices are estimated to be greater than the energy of two photons (707 kJ/mol) of a N_2 laser (laser most currently used for MALDI experiments), this two-photon ionization model cannot be assumed. When the lack of energy is quite low, ionization could nevertheless occur assisted by a thermal effect; it has been suggested as a "photothermal" mechanism [14].

Another ionization model, based on energy pooling, has also been proposed [15]. In this model, two or more separately excited matrix molecules pool their internal energy together to yield one matrix radical cation according to

$$\mathrm{MatMat} + nh\nu \rightarrow \mathrm{Mat^{*}Mat^{*}} \rightarrow \mathrm{Mat} + \mathrm{Mat}^{+\cdot} + e^{-} \tag{2}$$

Zenobi and Knochenmuss point out many arguments in favor of this mechanism [1]. "Energy pooling" and

Table 1
UV-LDI mass spectra of DHB at four values of laser energy; relative abundances were determined from the ion peak areas; they are given as percentages of the base peak area

	Laser energy (μJ)			
Ions	18	19	20	22
Positive ions				
MNa^+ (*m/z* 177)	40	25	11	46
$[MH_2]^{\cdot+}$ (*m/z* 156)	...	18	14	17
MH^+ (*m/z* 155)	100	100	72	51
$[M]^{\cdot+}$ (*m/z* 154)	93	77	79	56
$[M - OH]^+$ (*m/z* 137)	74	57	100	67
$[M - H_2O]^{\cdot+}$ (*m/z* 136)	...	...	37	100
Negative ions				
$[M]^{\cdot-}$ (*m/z* 154)	...	24	21	18
$[M - H]^-$ (*m/z* 153)	100	100	100	67
$[M - H_2]^{\cdot-}$ (*m/z* 152)	...	54	83	100
$[M - CHO_2]^-$ (*m/z* 109)	...	...	...	13
$[M - CH_2O_2]^{\cdot-}$ (*m/z* 108)	...	...	...	16

photothermal processes are usually assumed to coexist in MALDI experiments.

Mechanisms proposed above do not take into account the formation of Mat$^{\cdot\,-}$ radical anions nor that of MatH$^+$ and [Mat$-$H]$^-$ pseudomolecular species which are currently displayed as matrix ions. Disproportionation reactions have been suggested to explain the simultaneous formation of positive and negative ions [16,17]. Such reactions consist in proton or electron transfer between two coupled molecules undergoing laser irradiation

$$\mathrm{MatMat} + nh\nu \rightarrow \mathrm{MatH}^+ + [\mathrm{Mat} - \mathrm{H}]^- \quad (3)$$

$$\mathrm{MatMat} + nh\nu \rightarrow \mathrm{Mat}^{+\cdot} + \mathrm{Mat}^{-\cdot} \quad (4)$$

A model involving an “excited-state proton transfer” (ESPT) has also been proposed to rationalize the formation of pseudomolecular ions [18]. It is well known that, in solution, the acidic properties of many aromatic derivatives are strongly enhanced when molecules are laser excited: absorption of only one photon allows a consequent decrease in their pK. Such a phenomenon could be responsible of proton transfer according to

$$\mathrm{Mat} + \mathrm{Mat}^* \rightarrow \mathrm{MatH}^+ + [\mathrm{Mat} - \mathrm{H}]^- \quad (5)$$

However, most of common matrices are not particularly ESPT-active neither in solution nor in the gas phase [12].

It is to be noticed that MALDI spectra are usually presented as the result of two successive ionization steps referred as “primary ion formation” and “secondary ionization reactions in the MALDI plume.” Both steps seem to be related to the physical properties (ionization energy, proton affinity,...) of gaseous molecules. However, where each one occurs is not clearly established.

3.3. Description and interpretation of mass spectra

The UV(337 nm)-LDI mass spectrum of DHB obtained in the positive mode was first described by Strupat et al. [19]. UV(337 nm)-LDI mass spectra of DHB in both positive and negative modes are presented in Table 1. LDI experiments were performed at four values of the laser fluence; an energy of 18 μJ corresponds to the threshold for ions to be observed.

At the threshold energy four ions appear in the positive mode: DHBNa$^+$ (*m/z* 177), DHBH$^+$ (*m/z* 155), DHB$^{+\cdot}$ (*m/z* 154) and [DHB$-$OH]$^+$ (*m/z* 137). A priori, the [DHB$-$OH]$^+$ ion may result from the loss either of the radical OH from DHB$^{+\cdot}$ or of water

Table 2
Electron impact spectra of DHB at 70 and 10 eV

Ions	*m/z*	EI 70 eV	EI 10 eV
$M^{\cdot+}$	154	39	52
$[M - H_2O]^{\cdot+}$	136	100	100
$[M - H_2O - CO]^{\cdot+}$	108	54	18
$[M - H_2O - 2CO]^{\cdot+}$	80	68	15

from DHBH$^+$. To give an insight on it, the electron impact mass spectra of DHB were recorded at 10 and 70 eV; they are reported in Table 2. Even at the high energy value of 70 eV, any loss of OH is observed from DHB$^{+\cdot}$; the formation of [DHB−OH]$^+$ in MALDI is thus attributed to the loss of water from the protonated molecule. At energies above the threshold, a reduced form of the molecular radical cation ([DHBH^2]$^{\cdot+}$, *m/z* 156) is observed. At more higher energies, DHB$^{+\cdot}$ loses water to give *m/z* 136, as observed in the EI spectra.

In the negative mode, at low fluence, only [DHB−H]$^-$ (*m/z* 153) is observed. The radical anion DHB$^{\cdot-}$ (*m/z* 154) appears at higher laser fluences as well as the fragment ion [DHB−H$_2$]$^{\cdot-}$ (*m/z* 152). Two fragment ions (*m/z* 109 and *m/z* 108) involving the loss of the carboxylic function are observed at the highest laser irradiance. The formation of DHB$^{\cdot-}$ at a higher fluence than [DHB−H]$^-$ could be very informative. Recently, Karas et al. have presented the neutralization of some multi-charged species formed in MALDI as the result of electron capture [20]. Free electrons are detected in all the negative MALDI spectra but it is well known that capture of an electron by a molecule requires “threshold electrons” with very small kinetic energies. As DHB$^{\cdot-}$ ions are not observed at the threshold fluence where few species are desorbed, it may be concluded that the electron capture phenomenon depends on the pressure and thus occurs more probably in the plume than in the solid phase. Assuming this point, this result also suggests that, at higher fluences, the species in the plume are thermalyzed enough so that a thermodynamical equilibrium could be reached. This is in agreement with recent considerations of Knochenmuss et al. stating that “knowledge or calculation of quantitative reaction data leads increasingly toward the hypothesis that UV/MALDI mass spectra are largely thermochemically predictable” [21]. The kinetic energy of matrix ions in the gas phase is given to be about 1 eV [22,23]. At this energy, collisions will only be reactive for reactions exothermic or low internal energy demanding. These reactions are most probably included in the so-called secondary ionization step, as suggested by Knochenmuss et al. [1,21].

3.4. Formation of DHB molecular and pseudomolecular ions

Evaluation of the energy associated with the formation of matrix ions imply to know characteristic thermochemical values such as the IE and the electron affinity (EA) of the neutral species, the PA of the neutral and deprotonated molecules. Most of the time, experimental values remain unavailable. In the case of DHB, the ionization energy [15] as well as the protonation [24–27] and deprotonation [16] energies were measured. We have thus chosen this example to test the reliability of the B3LYP density functional approach in evaluating thermochemical characteristics of MALDI matrices. The calculated ionization energies are deduced from the total energies of the most stable neutral and ionized forms of the molecule.

The stablest structures describing DHB (**1**), DHB$^{\cdot+}$ (**2**), DHB$^{\cdot-}$ (**3**) and DHBH$^+$ (**4**) are presented in Fig. 1, as well as three structures for [DHB−H]$^-$ (**5**–**7**). Many structures and conformers were optimized to describe both DHBH$^+$ and [DHB−H]$^-$ ions. Protonation has been considered on the four oxygen atoms of the molecule and even on the aromatic ring; the resulting optimized geometries will be displayed in a future publication. The most stable form of DHBH$^+$ (**4**) results from protonation of the carbonyl oxygen and is stabilized by hydrogen bonding between the protonating hydrogen and the oxygen atom of the 2-OH function. Deprotonation of either the carboxylic function or the 2-hydroxylic group leads to the most stable [DHB−H]$^-$ structures (**5**, **6**) which differ by only 1 kJ/mol so that it cannot be concluded in favor of one of them. The third structure (**7**) resulting from deprotonation of the 5-hydroxylic group is taken into account because it will be consid-

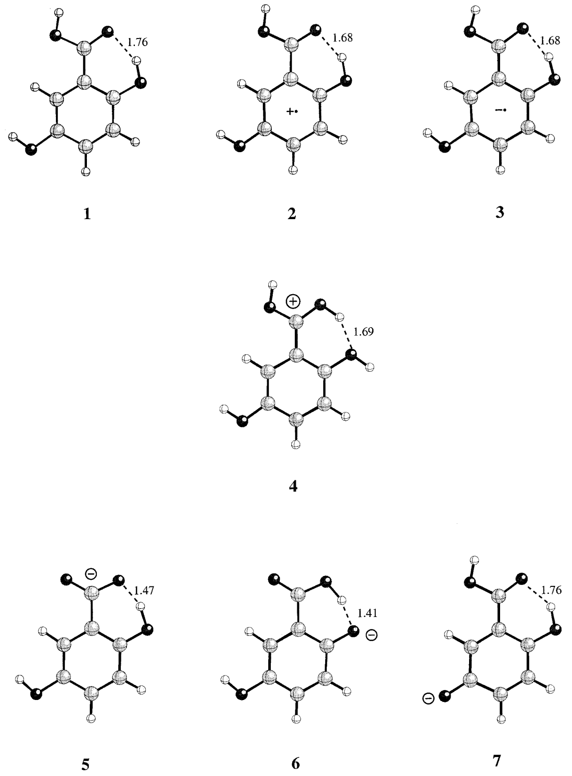

Fig. 1. B3LYP-6-31G** optimized geometries of the most stable structures of DHB (**1**), DHB $^{\cdot +}$ (**2**), DHB $^{\cdot -}$ (**3**), DHBH^{+} (**4**) and of the most probable structures of [DHB-H]- (**5**-**7**).

ered in bimolecular ionization mechanisms (see the following). The total energies E of all these species are tabulated in Table 3. The ionization enthalpies of DHB in the gas phase were deduced from the total energies of the most stable structures and reported in Table 4 where they are compared with the corresponding experimental values. For the ionization energy as well as for the proton affinity of the neutral and deprotonated molecule, Table 4 shows an excellent agreement between the experimental and calculated values. As a matter of fact, the discrepancy between the experimental and calculated values does not exceed 2.5%. Earlier semiempirical calculations led to (Koopman) IE values close to 870 kJ/mol, i.e. about 100 kJ/mol higher than the experimental value [15]. Ab initio calculations at the 4-31G level of theory gave IE(DHB)=824 kJ/mol, a value lower than the preceding ones but still too high. In our knowledge, PA(DHB) has not been calculated. Concerning PA([DHB−H]$^{-}$), MOPAC semiempirical calculations are available and give 1439, 1383, and 1396 kJ/mol for DHB deprotonated on the carboxylic function and on the 2- and 5-hydroxyl groups, respectively [28]. The corresponding ab initio B3LYP values are 1361, 1361, and 1424 kJ/mol, respectively. In a general manner, the better agreement of our calculated values with the experimental results is due to the use a higher level of theory to describe the neutral and ionized DHB. Otherwise, we report a first estimation of the electron affinity of DHB: 54 kJ/mol.

These values were then used to evaluate the vari-

Table 3
Total energies (E in a.u.) evaluated at two levels of theory: SB = B3LYP-6-31+G(d,p) and LB = B3LYP-6-311+G(2d,2p) and thermal energies (E_{therm} in kJ/mol) of **1–7** and **9–13**; the total energy of the hydrogen atom is also given

Name	E_{SB}	$E_{\text{therm(SB)}}$	E_{LB}
DHB **1**	−571.314 021	350	−571.468 971
DHBH^{+} **4**	−571.648 688	383	−571.803 714
[DHB − H]$^{-}$ **5**	−570.782 778	311	−570.935 849
[DHB − H]$^{-}$ **6**	−570.781 839	309	−570.934 847
[DHB − H]$^{-}$ **7**	−570.757 747	309	−570.910 774
[DHB]$^{\cdot +}$ **2**	−571.025 503	351	−571.180 529
[DHB]$^{\cdot -}$ **3**	−571.330 745	340	−571.485 916
[DHB − H]· **9**	−570.670 849	316	−570.824 889
[DHB − H]· **10**	−570.676 197	316	−570.829 071
[DHBH$_2$]$^{\cdot +}$ **11**	−572.202 435	413	−572.358 253
[DHBH$_2$]$^{\cdot +}$ **12**	−572.159 028	413	. . .
[DHBH]· **13**	−571.850 399	375	−572.006 480
H·	−0.500 273	4	−0.502 156

Table 4
Calculated ΔE and experimental ionization ΔH_{exp} energies of DHB in kJ/mol; in the upper part of the table, ΔE correspond to thermochemical data such as IE (ionization energy), EA (electron affinity) or PA (proton affinity); in the lower part of the table, they correspond to the enthalpies of the reactions mentioned; ΔE were deduced from the total energies E of the most stable structures reported in Table 3 and were corrected for the thermal energies at 298 K determined at the lowest level of theory

Reaction	ΔE_{SB}	ΔE_{LB}	ΔH_{exp}
$\mathrm{IE}(\mathbf{1}) = E(\mathbf{2}) - E(\mathbf{1})$	758	758	777[a]
$\mathrm{EA}(\mathbf{1}) = E(\mathbf{1}) - E(\mathbf{3})$	34	34	...
$\mathrm{PA}(\mathbf{1}) = E(\mathbf{1}) - E(\mathbf{4})$	846	846	854[b]
$\mathrm{PA}(\mathbf{5}) = E(\mathbf{5}) - E(\mathbf{1})$	1356	1361	1359[c]
$\mathrm{PA}(\mathbf{6}) = E(\mathbf{6}) - E(\mathbf{1})$	1356	1361	...
$\mathrm{PA}(\mathbf{9}) = E(\mathbf{9}) - E(\mathbf{2})$	896	897	...
$\mathrm{PA}(\mathbf{10}) = E(\mathbf{10}) - E(\mathbf{2})$	882	888	...
$\Delta H(3a) = \mathrm{PA}(\mathbf{5}) - \mathrm{PA}\ (\mathbf{1}) = \mathrm{PA}(\mathbf{6}) - \mathrm{PA}(\mathbf{1})$	510	515	505[d]
$\Delta H(4a) = \mathrm{IE}(\mathbf{1}) - \mathrm{EA}(\mathbf{1})$	724	724	...
$\Delta H(6.1) = E(\mathbf{4}) + E(\mathbf{9}) - E(\mathbf{2}) - E(\mathbf{1})$	50	53	...
$\Delta H(6.2) = E(\mathbf{4}) + E(\mathbf{10}) - E(\mathbf{2}) - E(\mathbf{1})$	36	42	...
$\Delta H(7.1) = -\mathrm{EA}(\mathbf{9}) = E(\mathbf{6}) - E(\mathbf{9})$	−284	−282	...
$\Delta H(7.2) = -\mathrm{EA}(\mathbf{10}) = E(\mathbf{7}) - E(\mathbf{10})$	−207	−207	...
$\Delta H(8.1) = E(\mathbf{11}) + E(\mathbf{9}) - E(\mathbf{4}) - E(\mathbf{1})$	231	231	...
$\Delta H(8.2) = E(\mathbf{11}) + E(\mathbf{10}) - E(\mathrm{A}) - E(\mathbf{1})$	217	220	...
$\Delta H(9) = -\mathrm{EA}(\mathbf{4}) = E(\mathbf{13}) - E(\mathbf{4})$	−518	−521	...
$\Delta H(10) = E(\mathbf{11}) + E(\mathbf{5}\text{ or }\mathbf{6}) - E(\mathbf{13}) - E(\mathbf{1})$	472	478	...
$\Delta H(11) = E(\mathbf{11}) + E(\mathbf{10}) - E(\mathbf{13}) - E(\mathbf{2})$	−13	−7	...
$\Delta H(12) = E(\mathbf{11}) + E(\mathbf{1}) - E(\mathbf{13}) - E(\mathbf{4})$	−51	−50	

[a] See [15].
[b] See [27].
[c] ΔH is estimated to be about 30 kJ/mol higher (typical entropy contribution at 300 K) than the experimental ΔG value from [16].
[d] ΔH is estimated from values of [16] and [27].

ations of enthalpy associated with the reactions proposed as ionization models under laser irradiation. The variations of enthalpy of the reactions related to the formation of DHBH^+ with $[\mathrm{DHB-H}]^-$ and of $\mathrm{DHB}^{\cdot +}$ with $\mathrm{DHB}^{\cdot -}$ in the gas phase, following:

$$\mathrm{DHB_{gas}} + \mathrm{DHB_{gas}} \rightarrow \mathrm{DHBH^+_{gas}} + [\mathrm{DHB - H}]^-_{\mathrm{gas}} \tag{3a}$$

$$\mathrm{DHB_{gas}} + \mathrm{DHB_{gas}} \rightarrow \mathrm{DHB^{+\cdot}_{gas}} + \mathrm{DHB^{-\cdot}_{gas}} \tag{4a}$$

were calculated to be 515 and 724 kJ/mol, respectively. The calculated enthalpy of reaction (3a) is in quite agreement with that deduced from experimental values which is 505 kJ/mol [16,27].

The energy associated with

$$\mathrm{DHB_{gas}} + \mathrm{DHB^*_{gas}} \rightarrow \mathrm{DHBH^+_{gas}} + [\mathrm{DHB - H}]^-_{\mathrm{gas}} \tag{5a}$$

in the gas phase was also evaluated. ΔH (5a)$=$ $\Delta H_{\mathrm{acid}}(\mathrm{DHB^*}) - \mathrm{PA(DHB)}$. As $\Delta H_{\mathrm{acid}}(\mathrm{DHB^*})$ is not known, it was approximated to be in between $\Delta H_{\mathrm{acid}}(\mathrm{DHB})$ and $\Delta H_{\mathrm{acid}}(\mathrm{DHB}^{\cdot +})$. $\Delta H_{\mathrm{acid}}(\mathrm{DHB}) = \mathrm{PA}(\mathbf{5}) = \mathrm{PA}(\mathbf{6}) = 1361$ kJ/mol. $\Delta H_{\mathrm{acid}}(\mathrm{DHB}^{\cdot +})$ is evaluated as $E(\mathbf{10}) - E(\mathbf{2}) = 888$ kJ/mol. Consequently, $\Delta H_{\mathrm{acid}}(\mathrm{DHB^*})$ was approximated as 1125 kJ/mol. Combining this value with PA(DHB) leads to ΔH (5a)$=$279 kJ/mol. Assuming the kinetic energy of species in the plume, the enthalpies of reactions (3a), (4a), and (5a) are too high to expect their occurrence in the gas phase.

On a thermochemical point of view, may some reactions occur in the gas phase? The answer is dramatically depending on the species present in the plume: molecular and pseudomolecular ions, fragment ions, electrons, etc. In agreement with what is observed at the threshold, we start with the assump-

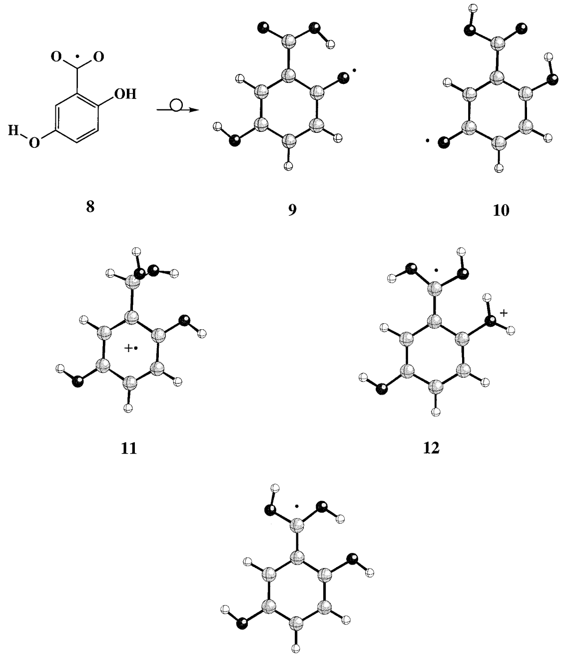

8 9 10

11 12

13

Fig. 2. Structures of radicals [DHB-H]$^{\cdot}$ (**9-10**), [DHB+H]$^{\cdot}$ (**13**) and of radical cation [DHB+2H]$^{\cdot+}$ (**11,12**).

tion that some DHB$^{\cdot+}$, DHBH^{+} and [DHB−H]$^{-}$ are already formed when entering the plume. By collision with neutral molecules, these ions may undergo reactions such as the deprotonation of radical cations

$$\mathrm{DHB}^{\cdot+} + \mathrm{DHB} \rightarrow \mathrm{DHBH}^{+} + [\mathrm{DHB} - \mathrm{H}]^{\cdot} \tag{6}$$

which can be followed by electron attachment on [DHB−H]$^{\cdot}$ [1,20]

$$[\mathrm{DHB} - \mathrm{H}]^{\cdot} + e^{-} \rightarrow [\mathrm{DHB} - \mathrm{H}]^{-} \tag{7}$$

The energetics associated with the formation of DHBH^{+} and [DHB−H]$^{-}$ ions are evaluated according to both reactions (6) and (7). The evaluation of EA([DHB−H]$^{\cdot}$) is depending on the proton lost from [DHB]$^{\cdot+}$ in reaction (6). It is well known by H/D exchange experiments that the protonating hydrogen is labile. Three hydrogen are labile in [DHB]$^{\cdot+}$: the carboxylic one and both hydroxylic hydrogens on C_2 and C_5. The corresponding deprotonated structures **8**, **9**, and **10** are displayed on Fig. 2. Geometry optimization of **8** straight led to **9**. Considering the initial state of reaction (6), the carbonyl function of the neutral molecule may be protonated by either the hydroxylic hydrogen on C_2 or on C_5 of the radical cation, depending on the geometrical orientation of both species. The activation energies of reaction (6.1) leading to the formation of **4** and **9** and of reaction (6.2) associated with the formation of **4** and **10** are 53 and 42 kJ/mol, respectively. The exothermicity of (7) is depending on the electron affinity of [DHB−H]$^{\cdot}$. EA(**9**) and EA(**10**) were calculated to be 282 kJ/mol and 207 kJ/mol, respectively. Since reaction (6) is very easy (about 50 kJ/mol) and reaction (7) is exothermic, there is a great probability for these reactions to occur in the plume. In presence of an analyte M with a PA greater than that of DHB, reaction (6) may become exothermic, in accordance with what is generally observed in MALDI experiments where MH^{+} is often the base peak of the spectra. Moreover, the fact that **8** straight led to **9** tends to show that **9** is more stable than **8**, **10** being the most stable geometry. Assuming reactions (6) and (7) as a probable mechanism for protonation/deprotonation of the matrix and/or the analyte, our theoretical results on [DHB−H]$^{\cdot}$ species may rationalize the fact, well-known by MALDI users, that the presence of hydrolic groups on the aromatic ring significantly increases the efficiency of the matrix [29].

3.5. Reduction of DHB molecular ions

We propose models attempting to explain the formation of [DHBH$_2$]$^{\cdot+}$. It has been shown earlier that reduction of conjugated carbonyl groups leads to [M+2H]$^{\cdot+}$ and [M+3H]$^{+}$ ions in NH_3−CI experiments [30] and to [M+2H]$^{\cdot+}$ under MeV ion bombardment [31]. In these works, H/D exchange showed that the transferred hydrogen are labile but the reduction mechanism remains much debated. In our experiments, any [DHB+3H]$^{+}$ is observed (the *m/z* 157 ion is not reported in Table 1 since its relative abundance is less than 1.5% and corresponds to the ^{13}C isotopic contribution of *m/z* 156) and the reduced radical cation [DHBH$_2$]$^{\cdot+}$ does not appear at the threshold but is formed at higher laser fluences. This is an important argument to postulate that, as for $DHB^{\cdot-}$, thermalization is a determining factor in the formation of this ion, in agreement with a reaction occurring in the gas phase. Several reactions are proposed to explain the formation of $[DHBH_2]^{\cdot+}$. The first hypothesis involves $DHBH^+$ and DHB

$$DHBH^+ + DHB \rightarrow DHBH_2^{\cdot+} + [DHB - H]^{\cdot} \quad (8)$$

Both structures **11** and **12** were chosen to describe $[DHBH_2]^{\cdot+}$. **11** is a radical cation in which the carbonyl function has been reduced. **12** is a distonic radical cation (Fig. 2). Geometry optimization gives **11** more stable than **12** by 114 kJ/mol (Table 3). Consequently, the formation of **12** is not expected. The enthalpy of reaction (8) is calculated to be 231 or 220 kJ/mol, according to the structure of the $[DHB-H]^{\cdot}$ radical involved in the final state (**9** or **10**, respectively). Other mechanisms involve as first step the reduction of $DHBH^+$ by electron capture

$$DHBH^+ + e^- \rightarrow DHBH^{\cdot} \quad (9)$$

to give the radical **13**. This radical may react either with a DHB molecule

$$DHBH^{\cdot} + DHB \rightarrow DHBH_2^{\cdot+} + [DHB - H]^- \quad (10)$$

or with a cation

$$DHBH^{\cdot} + DHBH^{\cdot+} \rightarrow DHBH_2^{\cdot+} + [DHB - H]^{\cdot} \quad (11)$$

$$DHBH^{\cdot} + DHBH^+ \rightarrow DHBH_2^{\cdot+} + DHB \quad (12)$$

An electron capture as first step is in good agreement with the appearance of $[DHBH_2]^{\cdot+}$ at the same laser fluence than $DHB^{\cdot-}$.

The enthalpies of reactions (10), (11), and (12) were calculated to be +440, −7 and −50 kJ/mol, respectively. The great endothermicity of reaction (10) may be compensated by the internal energy acquired by the radical during electron capture ($\Delta H(9) = -521$ kJ/mol). Reactions (11) and (12) are thermochemically favored but statistically less probable than reaction (10) since the molecules/ions ratio is assumed to be about 10^4 in the plume.

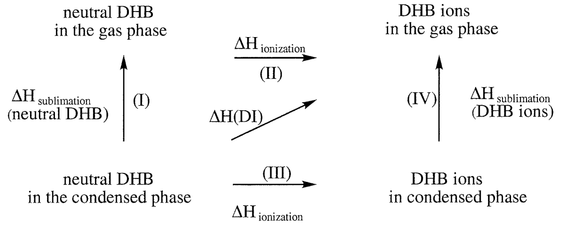

Fig. 3. Thermochemical diagram of desorption-ionization (DI).

3.6. Desorption-ionization (DI) model

In summary, we have shown on thermochemical criteria that several reactions: (6), (7), (9), (10), (11), and (12) may occur under collisions in the gas phase. Taking into account the differences observed on LDI spectra at different laser fluences, it is clear that $DHB^{\cdot-}$ and $[DHBH_2]^{\cdot+}$ are formed in the gas phase after thermalization of electrons. In counter part, the endothermicity of reactions (1), (2), (3a), (4a), (5a), and (8) prevents them from occurring in the gas phase. Given the appearance of $DHB^{\cdot+}$, $DHBH^+$ and $[DHB-H]^-$ at the threshold, it is likely that some of these ions are straight formed in the condensed state (primary ionization). In such conditions, the energy required to observe $DHBH^+$ and $[DHB-H]^-$ ions, on one hand, and $DHB^{\cdot+}$ ions, on the other hand, can be evaluated via a thermochemical cycle taking into account not only the ionization energies but also the sublimation energies (Fig. 3).

The energy (ΔH(DI)) required to transform neutral molecules of DHB in the condensed state into gaseous DHB ions may be evaluated in two different manners: (1) adding the ionization energy of molecules in the gas phase (ΔH(II)) to the sublimation energy (ΔH(I)) of condensed molecules or (2) summing the ionization energy in the condensed phase (ΔH(III)) and the sublimation energy of ionic species (ΔH(IV)). ΔH(DI) can only be estimated following the pathway (1) because ΔH(III) and ΔH(IV) are unknown. The sublimation energies are given by mole of desorbed species and are thus depending on the number of species involved in each reaction. Since most of the proposed models involve bimolecular reactions, the following reaction is considered as an example:

$$\mathrm{DHB_{solid}} + \mathrm{DHB_{solid}} \rightarrow \mathrm{DHB_{gas}} + \mathrm{DHB_{gas}}$$
$$\rightarrow \mathrm{DHBH^{+}_{gas}} + [\mathrm{DHB} - \mathrm{H}]^{-}_{\mathrm{gas}} \qquad (13)$$

We propose a simple thermochemical diagram showing evidence that MALDI is a very energy demanding process and that differences in efficiency between matrices should be related to their chemical structures rather than to their physical properties.

According to reaction (13), the sublimation energy of DHB will be considered two times. The sublimation energy of DHB may be approximated to be close to that of p-hydroxybenzoic acid, i.e. about 120 kJ/mol [32]. In these conditions, the $\Delta H(\mathrm{DI})$ associated with reaction (13) is $\Delta H(\mathrm{DI}) \approx (2\times120)+505 \approx 745$ kJ/mol. If we now consider that both neutral molecules of DHB are sublimated coupled together (as postulated in disproportionation mechanisms) the sublimation energy of the couple can be approximated as at least the half of the preceding one, i.e. 120 kJ/mol. Nevertheless, the variation of enthalpy associated with reaction (13) remains very high: $\Delta H(\mathrm{DI}) \approx 120+505 \approx 625$ kJ/mol.

The energy required to observe $\mathrm{DHB}^{\cdot +}$ ions depends on the ionization reaction assumed. If a photothermal ionization pathway (see reaction (2)) is considered, $\Delta H(\mathrm{DI})$ can be approximated from

$$2\,\mathrm{DHB_{solid}} \rightarrow 2\,\mathrm{DHB_{gas}} \rightarrow \mathrm{DHB_{gas}} + \mathrm{DHB^{\cdot +}_{gas}} \qquad (14)$$

as the sum of the ionization energy of DHB and the enthalpy variation required to sublimate two DHB molecules, i.e. $\Delta H(\mathrm{DI}) \approx 777+(2\times120) \approx 1017$ kJ/mol.

In both examples of ion formation, the sublimation energy of molecules remains relatively low compared to the energy required for ionization. On a thermochemical point of view, considering bimolecular reactions in disproportionation models only leads to diminuate the energy involved in the sublimation step; the energy required for the whole desorption-ionization process remains very high. Given the great demand in energy associated with desorption-ionization, the low differences in ionization energies as well as in sublimation energies from one matrix to another cannot rationalize their differences in MALDI efficiency. The differences in efficiency between matrices should be related to their chemical structures rather than to their physical properties.

4. Conclusions

This work shows that molecular orbital calculations performed with a B3LYP functional density approach can be accurate to evaluate thermochemical data on molecules with several heavy atoms: our calculation results differ by less than 2.5% from experimental determinations. We estimated the electron affinity of DHB at 54 kJ/mol. We showed evidence of two equivalent deprotonation sites on neutral DHB: the carboxylic function and the 2-hydroxyl group. Considering bimolecular proton-exchange reactions, it is important to note that the hydrogen atom on the 5-hydroxyl group is the most acid of the $\mathrm{DHB}^{\cdot +}$ radical cation. Such results give a possible explanation of the great role played by the hydroxylic substituants in the particular efficiency of DHB as a MALDI matrix. The well-founded ionization models usually postulated from LDI and MALDI experiments were evaluated on thermochemical basis. It allowed us to give an insight on reactions, which are thermochemically the most probable in the solid state and in the gas phase. The observation of gaseous molecular ions in LDI and MALDI experiments has been shown to be a very energy-demanding process.

References

[1] R. Zenobi, R. Knochenmuss, Mass Spectrom. Rev. 17 (1998) 337.

[2] B.J. Smith, L. Radom, J. Phys. Chem. 99 (1995) 6468.

[3] B.J. Smith, L. Radom, Chem. Phys. Lett. 245 (1995) 123.

[4] I.A. Topol, S.K. Burt, N. Russo, M. Toscano, J. Am. Soc. Mass Spectrom. 10 (1999) 318.

[5] D. Yu, A. Rauk, D.A. Armstrong, J. Am. Chem. Soc. 117 (1995) 1789.

[6] A.D. Becke, J. Chem. Phys. 98 (1993) 5648.

[7] P. Burk, I. A. Koppel, I. Koppel, I. Leito, O. Travnikova, Chem. Phys. Lett. 323 (2000) 482.

[8] GAUSSIAN94 (Revision B.1), M.J. Frisch, G.W. Trucks, H.B. Schlegel, P.M.W. Gill, B.G. Johnson, M.A. Robb, J.R. Cheeseman, T.A. Keith, G.A. Petersson, J.A. Montgomery, K. Raghavachari, M.A. Al-Laham, V.G. Zakrzewski, J.V. Ortiz, J.B. Foresman, J. Cioslowski, B.B. Stefanov, A. Nanayakkara,

M. Challacombe, C.Y. Peng, P.Y. Ayala, W. Chen, M.W. Wong, J.L. Andres, E.S. Replogle, R. Gomperts, R.L. Martin, D.J. Fox, J.S. Binkley, D.J. Defrees, J. Baker, J.J.P. Stewart, M. Head-Gordon, C. Gonzalez, J.A. Pople, Gaussian, Inc., Pittsburgh, PA, 1995.

[9] A. Vertes, G. Irinyi and R. Gijbels, Anal. Chem. 65 (1993) 2389.

[10] R.E. Johnson, Int. J. Mass Specrom. Ion Processes 139 (1994) 25.

[11] L.V. Zghigilei, B.J. Garrison, Appl. Phys. Lett. 74 (1999) 1341.

[12] H. Eyring, M. Karas, F. Hillenkamp, Org. Mass Spectrom. 27 (1992) 472.

[13] P.C. Liao, J. Allison, J. Mass Spectrom. 30 (1995) 408.

[14] D.A. Allwood, P.E. Dyer, R.W. Dreyfus, Rapid Commun. Mass Spectrom. 11 (1997) 499.

[15] V. Karbach, R. Knochenmuss, Rapid Commun. Mass Spectrom. 12 (1998) 968.

[16] K. Breuker, R. Knochenmuss, R. Zenobi, Int. J. Mass Spectrom. 184 (1999) 25.

[17] R. Knochenmuss, V. Karbach, U. Wiesli, K. Breuker, R. Zenobi, Rapid Commun. Mass Spectrom. 12 (1998) 529.

[18] M. Karas, D. Bachmann, F. Hillenkamp, Anal. Chem. 57 (1985) 2935.

[19] K. Strupat, M. Karas, F. Hillenkamp, Int. J. Mass Spectrom Ion Processes 111 (1991) 89.

[20] M. Karas, M. Glückmann, J. Schäfer, J. Mass Spectrom. 35 (2000) 1.

[21] R. Knochenmuss, A. Stortelder, K. Breuker, R. Zenobi, J. Mass Spectrom. 35 (2000) 1237.

[22] R.C. Beavis, B.T. Chait, Chem. Phys. Lett. 181 (1991) 479.

[23] Y. Pan, R.J. Cotter, Org. Mass Spectrom. 27 (1992) 3.

[24] R.J.J.M. Steenvoorden, K. Breuker, R. Zenobi, Eur. Mass Spectrom. 3 (1997) 339.

[25] R.D. Burton, C.H. Watson, J.R. Eyler, G.L. Lang, D.H. Pwell, M.Y. Avery, Rapid Commun. Mass Spectrom. 11 (1997) 443.

[26] T.J.D. Jorgensen, G. Bojesen, H. Rahbek-Nielson, Eur. Mass Spectrom. 4 (1998) 39.

[27] M. Mormann, S. Bashir, P. Derrick, D. Kuck, J. Am. Soc. Mass Spectrom. 11 (2000) 544.

[28] Y. Huang, D.H. Russell, Int. J. Mass Spectrom. 175 (1998) 187.

[29] M. Karas, U. Bahr, J.R. Stah-Zeng, in Large Ions: Their Vaporization, Detection and Structural Analysis, T. Baer, C.Y. Ng, I. Powis (Eds.), Wiley, London, 1996, p 27.

[30] K.P. Maddhusudanan, V. Screenivas Murthy, D. Fraisse, Org. Mass Spectrom. 22 (1987) 665.

[31] J. P. Denhez, Eur. Mass Spectrom. 1 (1995) 141.

[32] Handbook of Chemistry and Physics, 69th ed., R.C. Weast (Ed.), CRC Press, Boca Raton, FL, 1988–89, pp. C664–665.